ENGLISH VERSION

Compressive strength of concrete made with electric arc furnace slag and recycled ground glass as replacement of coarse and fine aggregate

Resistencia a compresión de concreto con escoria de horno de arco eléctrico y vidrio molido reciclado en remplazo del agregado grueso y fino

Yasmín Andrea Rojas [*,1] https://orcid.org/0000-0002-4237-4604
Enrique Vera López [**] https://orcid.org/0000-0003-4150-9308

[*] Group on Integrity and Materials Evaluation GIEM, Boyacá, Colombia
[**]Universidad Pedagógica y Tecnológica de Colombia, Boyacá, Colombia

Fecha de Recepción: 13/03/2021
Fecha de Aceptación: 27/09/2021
PAG 342-360

Abstract

Concrete is one of the most studied industrial products with the aim of improving its durability, strength, and workability, as well as developing innovative alternatives in its production to reduce the environmental footprint (Rivera, 2013). This research validates the use of industrial waste generated in the department of Boyacá - Colombia, within the production of concrete for the construction of rigid pavements. The research followed several stages, beginning with the physical, chemical, and mechanical characterization of the materials and the design of the standard mixture following the ACI 211 methodology. Subsequently, the 25%, 50%, 75%, and 100% of the gravel was replaced by electric arc furnace slag (EAFS), and 20, 30 and 40% of the sand by the recycled ground glass (RGG). Finally, the compressive strength of the concrete mixtures was analyzed.

Keywords: EAFS; concrete; compression strength; recycling glass; rigid pavement

Resumen

El concreto es uno de los productos industriales más estudiado anualmente con el ánimo de mejorar su durabilidad, resistencia y trabajabilidad, así como alternativas innovadoras en su producción que reduzcan la huella ambiental (Rivera, 2013). La presente investigación busca validar el uso de desechos industriales generados en el departamento de Boyacá– Colombia, dentro de la producción de concretos para la construcción de pavimentos rígidos. La investigación siguió varias etapas, comenzando con la caracterización física, química y mecánica de los materiales y el diseño de la mezcla patrón siguiendo la metodología ACI 211. Posteriormente se reemplazó la grava por escoria de horno de arco eléctrico (EAFS) en los porcentajes de 25%, 50%, 75% y 100%, y la arena por vidrio molido reciclado (VMR) en los porcentaje de 20%, 30% y 40. Finalmente se analizó el comportamiento a la compresión simple de cilindros en las mezcla obtenidas.

Palabras clave: EAFS; concreto; resistencia a la compresión; vidrio reciclado; pavimento rígido

1. Introduction

Electric arc furnace slag (EAFS) and recycled ground glass (RGG) are waste produced from the steel industry and from the beverage industry, respectively.

EAFS has been investigated for decades as an aggregate (Adegoloye et al., 2016) and its use in the concrete production has increased considerably in the last years (Aprianti, 2016). The physical and chemical properties of EAFS have been evaluated, finding it suitable for use as concrete aggregates, due to its low absorption, guaranteeing better setting shrinkage and improvements in concrete durability (Sumayya et al., 2016).

Crystallized slag offers excellent adhesion properties to cement, volumetric stability, and durability, as well as greater fire resistance (Muhmood et al., 2009). Concretes with 100% gravel replaced by EAFS were found to be useful for construction (Rondi et al., 2016).

On the other hand, the increase on the population in urban centers has increased the generation of post-consumer glass waste in its main presentation, the glass bottle, which saturates landfills at a great rate, contaminating water sources due to their inadequate disposal (Ling et al., 2013).

[1] ***Corresponding author:***
Member of the research Group on Integrity and Materials Evaluation - GIEM– GIEM, Colombia
E-mail: yasmin.perez@uptc.edu.co

The use of RGG as replacement of fine aggregate in conventional concretes improves concrete workability, decreasing the amount of cement and water required on the mixtures (Nassar and Soroushian, 2012). Replacement of RGG by cement improves workability and increases the void content of the mix, while replacement of coarse aggregates by the RGG in concrete mixes decreases workability and the void content remains constant (Afshinnia and Rangaraju, 2016).

This research evaluated the compressive strength of concrete mixtures made with coarse and fine aggregates replacements by EAFS and RGG, respectively. Mix design of the studied concretes followed the ACI method, complemented with the use of the Fuller method (Gong et al., 2015); (Rajagopal et al., 1984) for the adjustment of the optimal curve in the gradation of the aggregates of the mix. The procedures and tests were carried out to follow the current regulations of the (INVIAS, 2012b) to guarantee that the results are iterative and reproducible.

2. Materials

2.1 Aggregates

The aggregates used in this research are divided into two groups: natural aggregates and by-products aggregates. The natural aggregates are gravel with a nominal maximum size of 0.019 m, from the Santa Lucia quarry in the municipality of Cucaita, and washed sand with a nominal maximum size of 0.00475 m from Alto del Moral in the municipality of Tunja.

The tests of hardness, durability, cleanliness, and geometry for the aggregates were carried out in accordance with the table 500-2 standard from the general specifications for road construction, (INVIAS, 2012a). (Table 1) shows the results in the laboratory tests carried out on the coarse aggregates, and their compliance to the reference value according to current regulations.

Table 1. Compliance to specifications from coarse aggregates (gravel and EAFS)

Characteristic	Reference	Result		COMPILANCE
		Gravel	EAFS	
HARDNESS				
Abrasion in the Los Angeles machine (gradation A), maximum (%). Standard E-218				
500 revolutions	40	36	20	Yes
Abrasion in the equipment Micro - Deval maximum (%). Standard E-238	30	24	7	Yes
Mechanical resistance by the method of 10% fines. Standard E-224				
Dry value, minimum (KN)	90	95	105	Yes
DURABILITY				
Sulfate soundness test (%). Standard E-220	20	2.46	1.66	Yes
CLEANLINESS				
Clay lumps and friables particles, maximum (%). Standard E-211	3.0	2.8		Yes
GEOMETRY (aggregate combinations e.g. 25% EAFS - 75% gravel)				
Percent of fractured particles. Standard E-227	60	90		Yes
Flat particles, elongated particles, maximum (%). Standard E-240	10	3.91		Yes

(Table 2) presents the compliance of the sand according to the INVIAS specification. (INVIAS, 2012a).

Table 2. Compliance to specifications from fine aggregates (Sand)

Characteristic	Reference	Result	COMPILANCE
DURABILITY			
Sulfate soundness test (%). Standard E-220	15	1.74	Yes
CLEANLINESS			
Clay lumps and friable particles, maximum (%). Standard E-211	3.0	0.8	Yes
Lightweight particles in aggregate, maximum (%). Standard E-221	0.5	-	-
Sand equivalent value, minimum (%). Standard E-133	60	64	Yes
Materials finer than 75 µm (No. 200), maximum (%). Standard E-214	3	2.8	Yes
Liquid limit, plastic limit, and plasticity index. Standards E-126, E-135	NP	NP	Yes

2.1.1 Recycled Ground Glass (RGG)

Glass is an amorphous material produced by melting silica, sodium carbonate, and calcium carbonate (CaCO3), followed by cooling, where solidification can occur without crystallization (Omran and Tagnit-Hamou, 2016).

The material used in this research was obtained from the collection at the source of the waste of transparent glass bottles, which were washed in a soapy solution, to remove labels and residues and then disinfected with an aqueous solution of chlorine at 0.1%. Subsequently, it was dried to a constant mass and manually crushed with the help of hammers. The material was ground in the Los Angeles machine for 10 minutes at 500 rpm. The glass produced after grinding was passed through the # 4 sieve. The retained material was reground for the same period of time and it was sieved again (Pérez et al., 2017).

The ground glass was observed with a scanning electron microscope to evaluate its morphology and structure. (Figure 1) shows the image of the RGG by SEM.

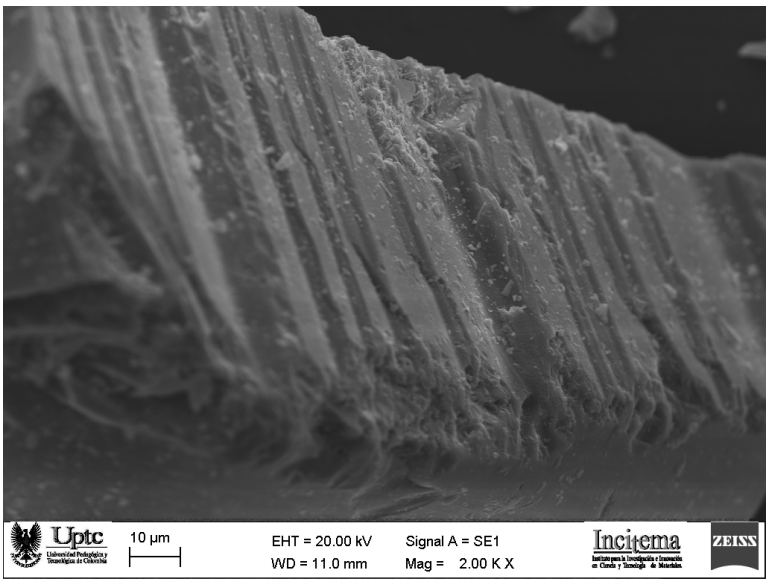

Figure 1. SEM image of RGG

(Figure 1) shows the twins presented in the glass particle during grinding. RGG is homogeneous in particle shape. The particles' size ranges between 1 and 3 µm, approximately.

2.2 EAFS

Electric Arc Furnace Slag (EAFS) is a by-product of the steel industry generated after melting and preliminary acid refining of liquid steel. It is a stone material that is easy to crush for use as a coarse aggregate in concrete mixtures. (Arribas et al., 2015).

The EAFS used for the research came from the DIACO steel company in Tuta, Boyacá – Colombia, and its chemical composition was determined by X-ray fluorescence (XRF) and X-ray diffraction (XRD). The obtained spectrum by XRF is shown in (Figure 2).

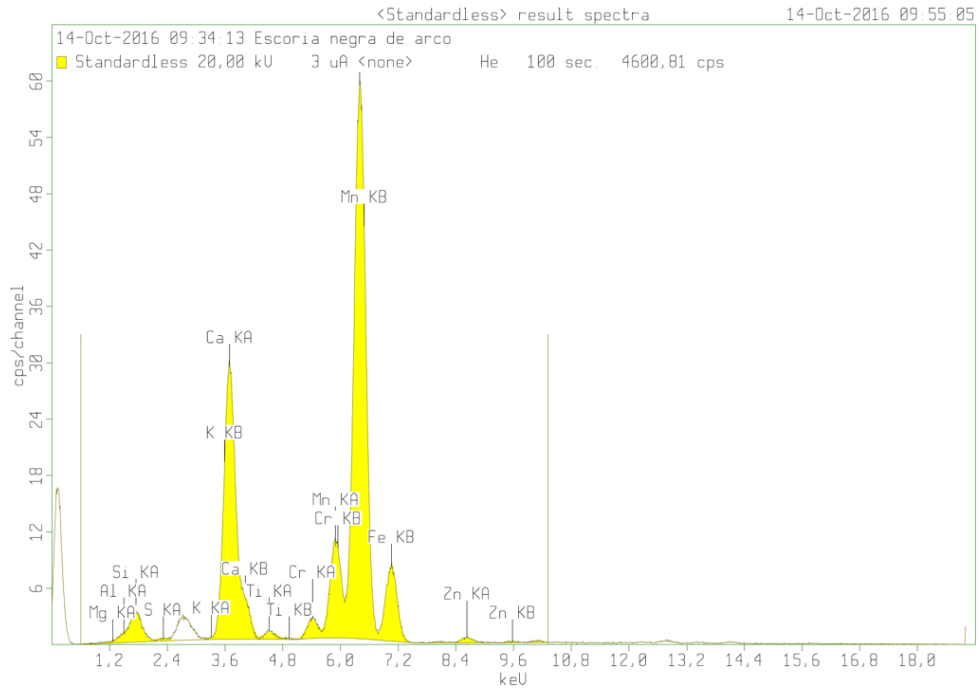

Figure 2. XRF Spectrum of EAFS.

Additionally, the EAFS was tested in XRD and the diffraction obtained spectrum indicated the presence of compounds associated with FeO in 24.9% and CaO in 75.1% (Pérez Rojas et al., 2021a). The obtained spectrum is shown in (Figure 3).

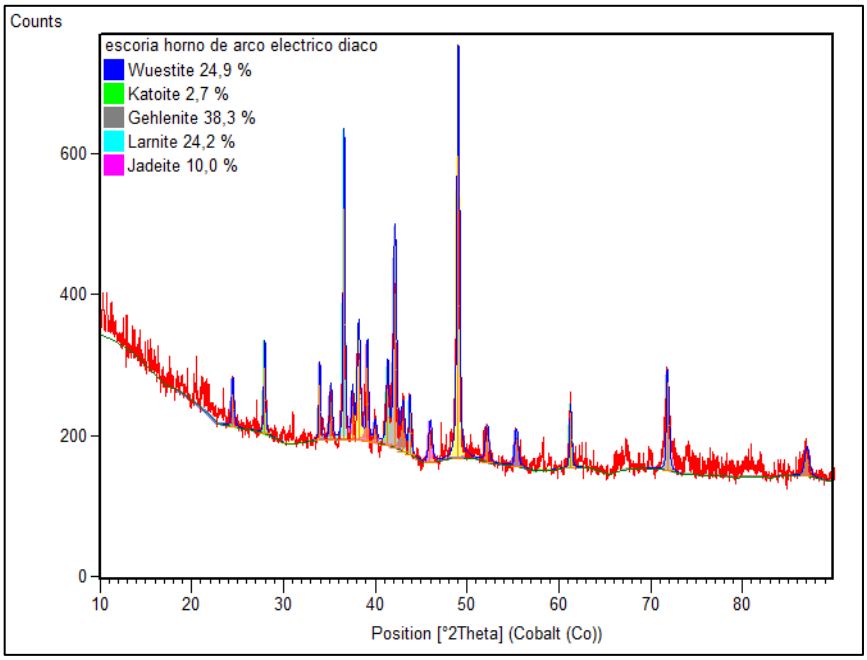

No.	Visi...	Ref. Code	Compound Na...	Chemical Form...	Score	Scale ...	Display Co...	Quality	Subfil...	Crystal System
1		96-900-8637	Wuestite	Fe4.00 O4.00	55	0,817	Blue	=	User I...	Cubic
2		96-900-2706	Katoite	Ca24.00 Al16.0...	16	0,396	Lime	=	User I...	Cubic
3		96-900-6114	Gehlenite	Ca4.00 Mg0.42...	55	0,720	Gray	=	User I...	Tetragonal
4		96-901-2790	Larnite	Ca8.00 Si4.00 ...	23	0,198	Aqua	=	User I...	Monoclinic
5		96-901-0470	Jadeite	Ca4.00 Fe4.00 ...	24	0,139	Fuc...	=	User I...	Monoclinic

Figure 3. DRX spectrum of EAFS.

3. Mixture design method

ACI 211.1 presents an empirical mixture design method widely confirmed by experimental information. The ACI 211.1 method is used when the aggregates meet the granulometric distribution (Romero and Hernández, 2014) and the consistency is used as a criterion for the selection of the slump (Giraldo Bolivar, 2006). ACI 211.1 method relates compressive strength to water-to-cement ratio (w/c) (Reddy et al., 2018).

The mixture design can be made by mixing the materials by absolute volume and then calculating the weights of each material used, or once the weight of a cubic meter of concrete is known, directly calculate the weight of each material incorporated in the mixture (Girardo Bolívar, 1987).

In the development of the mixture designs, the nine steps described by (Ávila Díaz et al., 2015), were followed, starting with the choice of the slump, the choice of the maximum aggregate size, the estimation of the air content, the estimation of the mixing water content, the selection of the w/c, the calculation of the cement dosage, the estimation of the aggregate proportions, the adjustment in humidity, and finally the adjustment in the test mixture.

(Table 3) presents the properties of the natural aggregates at the time of mixing the control mix.

Table 3. Material properties at the time of mixing

Type of aggregate	Description	Value
Gravel	Compacted unit weight Dry bulk density Absorption	1311 kg/m³ 2.29 g/cm³ 4.6 % 1.01%
Sand	Apparent density Absorption Fineness modulus	2.52 g/cm³ 1.5% 3.95% 2.4
Cement	Cement type ASTM C-1157 Specific weight	Portland cement type UG 3.15 g/cm³

4. Experimental design

The experimental design used in this research was a 4 x 3 x 3 factorial design. Three experimental factors where studied: the replacement of the coarse aggregate by EAFS (Factor A), which were 25, 50, 75, and 100%; the replacement the fine aggregate by RGG (Factor B), which were of 20, 30 and 40%; and age of testing (Factor C), which were 7, 28 and 56 days. 13 different mixtures were designed, including the standard mix (i.e., control mix). The designed mixtures are described in (Table 4), indicating the percentages of replacement by the alternative aggregates in each of the mixtures.

Table 4. Percentages of replacement by the alternative aggregates

Mix	***Coarse Aggregate***								***Fine Agrgregate***						
	Gravel (%)				*EAFS (%)*				*Sand (%)*				*RGG(%)*		
	100	*75*	*50*	*25*	*100*	*75*	*50*	*25*	*100*	*80*	*70*	*60*	*20*	*30*	*40*
Control	●								●						
M1		●						●		●			●		
M2		●						●			●			●	
M3		●						●				●			●
M4			●				●			●			●		
M5			●				●				●			●	
M6			●				●					●			●
M7				●		●				●			●		
M8				●		●					●			●	
M9				●		●						●			●
M10					●					●			●		
M11					●						●			●	
M12					●							●			●

4.1 Working formula

Following ACI 211.1 methodology, the amounts necessary for each batch of the mixtures were determined by weight. The initial design of the concrete mixture established a constant w/c of 0.47 for all the mixtures, but as a result of the slump adjustments and subsequent verification of the design strength, it was adjusted for each of the proposed mixtures. The w/c turned out to be equal per each EAFS replacement level. (Table 5) shows the proportions used in each of the mixtures and their respective w/c

Table 5. Working formulas for mixes per m3 of concrete

Materials	**Mix**												
	P1	M1	M2	M3	M4	M5	M6	M7	M8	M9	M10	M11	M12
water (kg)	271.6	271.9	258.0	253.2	244.6	261.4	271.6	254.4	242.3	242.4	233.9	227.8	229.7
Cement (kg)	602.0	602.7	584.1	550.5	596.5	637.5	662.4	591.7	563.5	563.8	497.7	484.7	488.8
Fine Aggregate (kg)	504.5	427.3	438.7	465.9	478.7	438.6	408.8	374.9	413.7	370.3	615.9	641.6	699.3
Coarse Aggregate (kg)	854.7	1037.0	1026.1	1019.5	1120.6	1160.9	1110.9	1140.8	1140.2	1140.9	1189.0	1224.6	1167.8
w/c Ratio	0.45	0.45			0.41			0.43			0.47		
Aggregate/ cement Ratio	2.3:1	2.5:1			2.5:1			2.7:1			3.8:1		

4.2 Compression Strength Analysis

Nine Cylinders of 10-cm diameter and 20-cm height for each mixture were casted and tested at 7, 28 and 56 days, following INVIAS E-410-07 (INVIAS, 2012b). The average strength of three specimens per age was recorded in MPa.

The results of the compressive strength of each mixture and age by percentage of replacement are shown in (Figure 4); (Figure 5); (Figure 6) and (Figure 7).

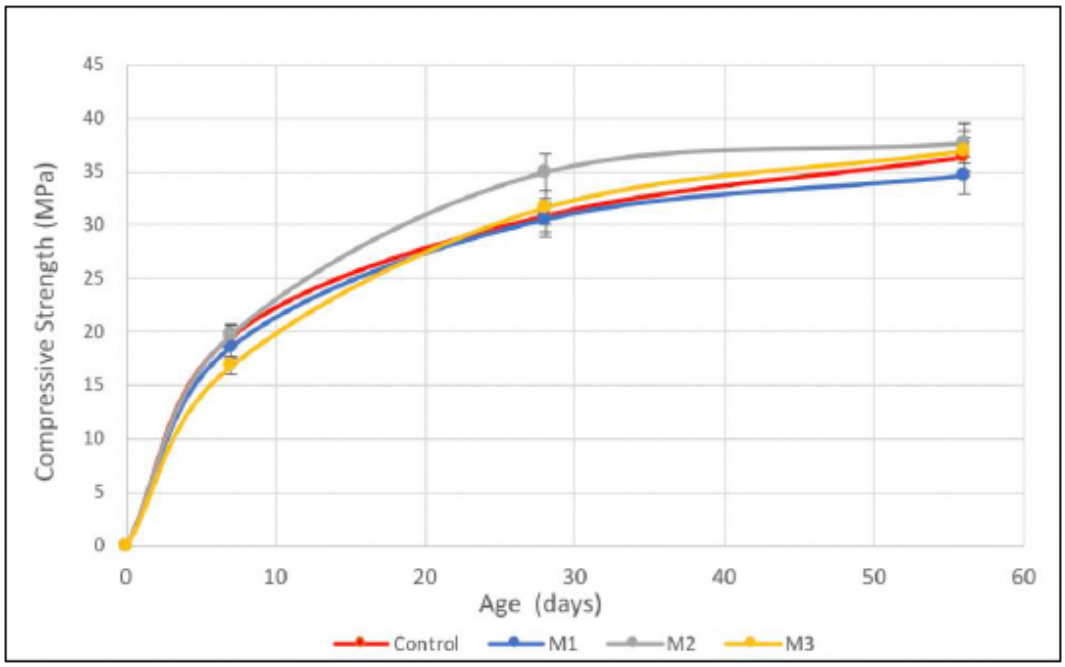

Figure 4. Compressive strength of replaced concrete mixes by 25% EAFS

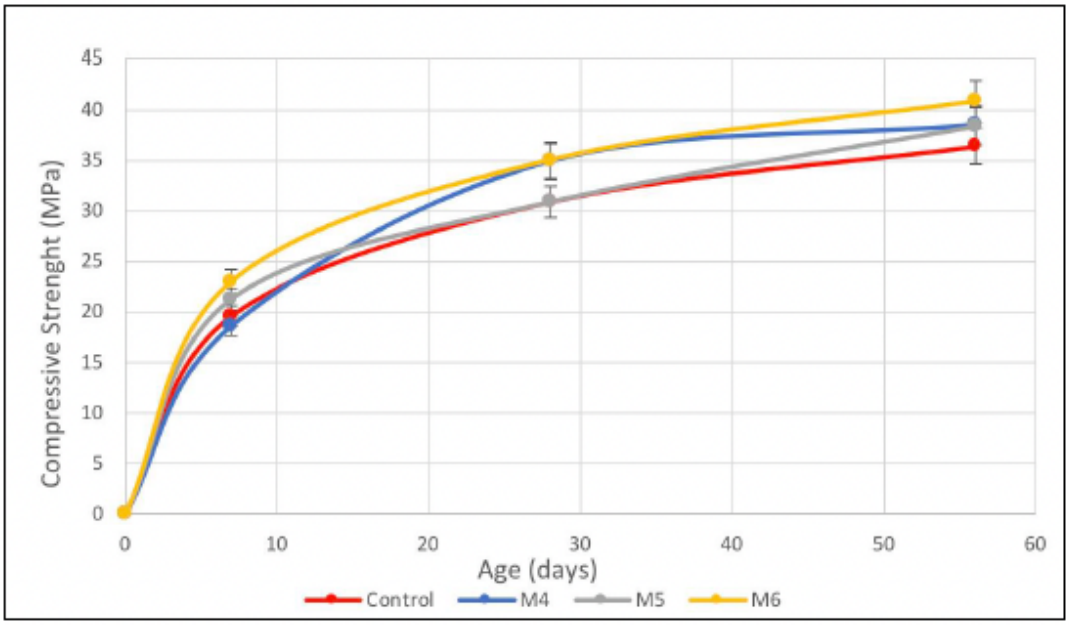

Figure 5. Compressive strength of replaced concrete mixes by 50% EAFS

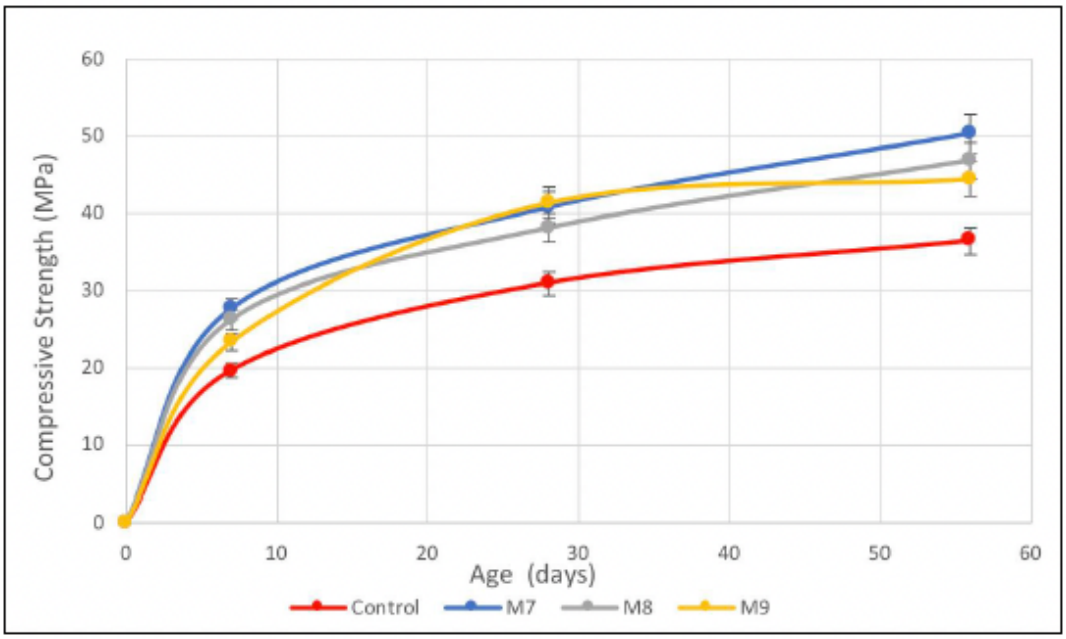

Figure 6. Compressive strength of replaced concrete mixes by 75% EAFS

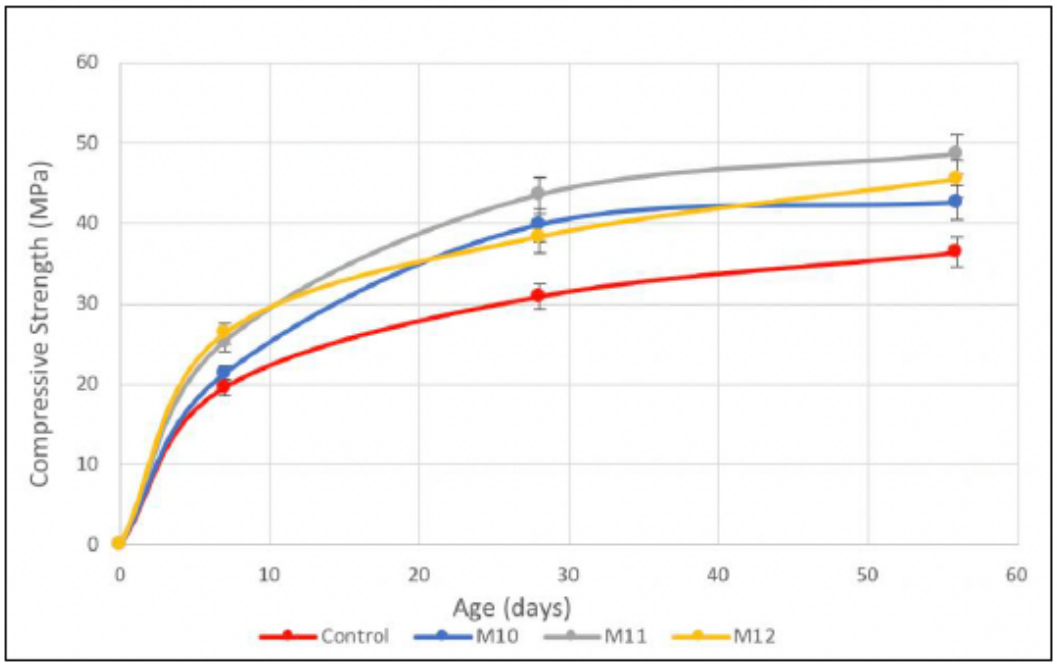

Figure 7. Compressive strength of replaced concrete mixes by 100% EAFS

4.3 Statistical analysis

The studied property was the compressive strength (MPa). The influence of the factors A, B and C, on the compressive strength measurements, were inferred by using the experimental design model.

(Figure 8), (Figure 9) and (Figure 10) are boxplot graphs and present the behaviour of the compressive strength taking into account the interaction between factors.

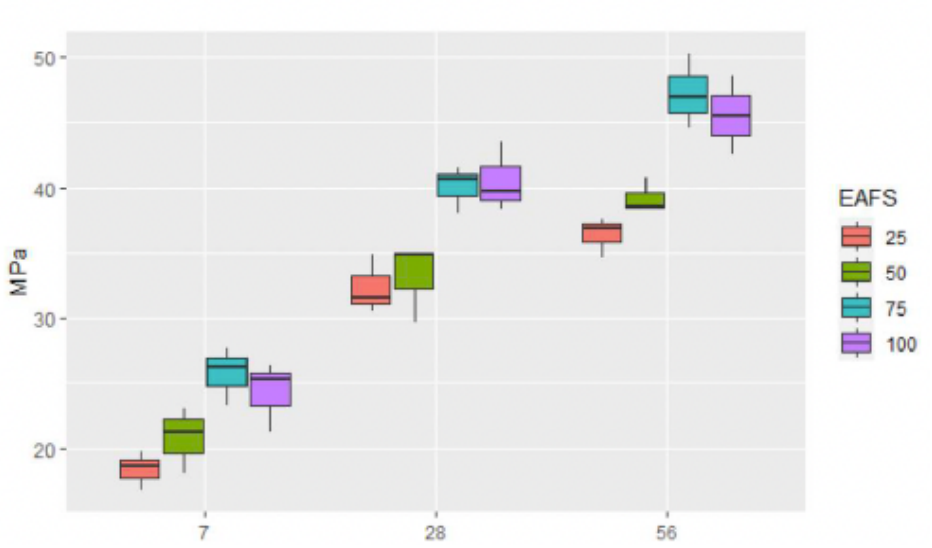

Figure 8. Compressive strength according to age and EAFS

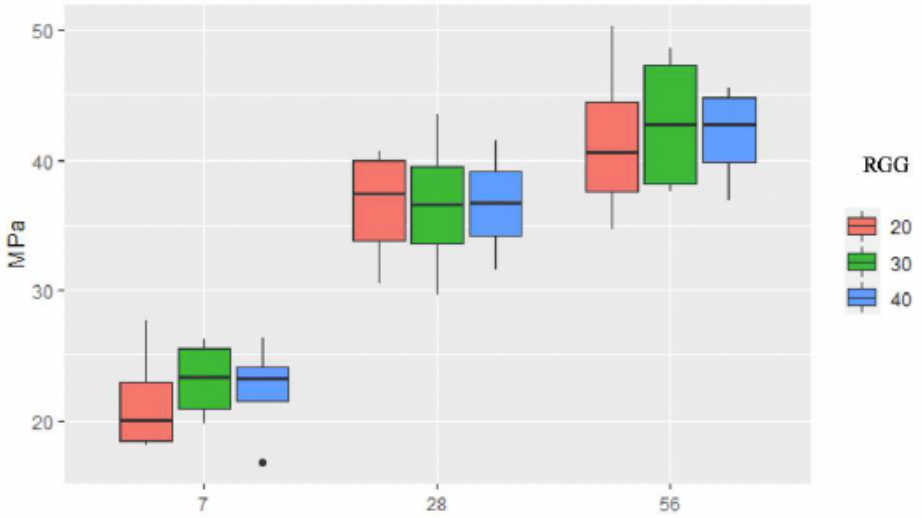

Figure 9. Compressive strength according to age and RGG

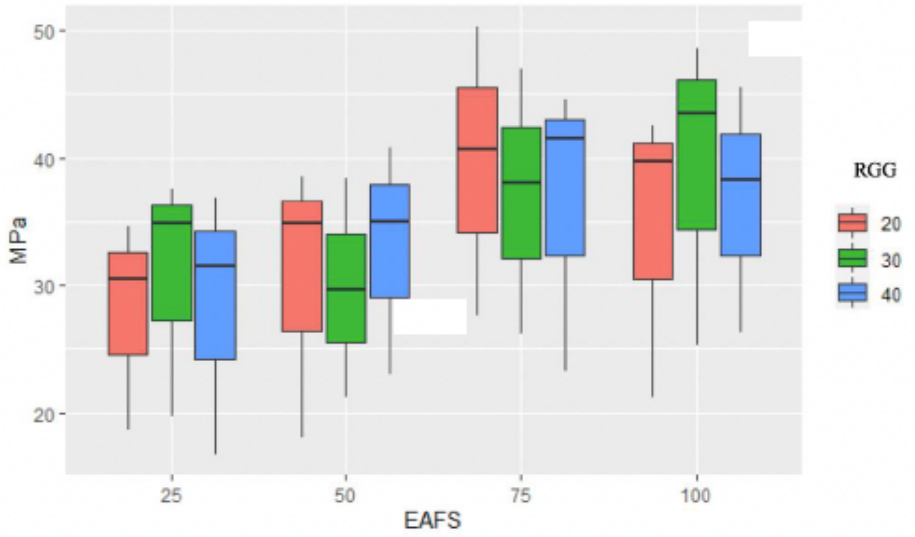

Figure 10. Compressive strength according to EAFS and RGG

(Figure 8) presents a difference between groups. Figure 9 and Figure 10 show no difference between the different factors and levels of compressive strength behavior. However, to be more conclusive, an analysis of variance (ANOVA) was carried out, considering each of the experimental factors and the interactions between them, which began by testing the model described in (Equation 1).
(Equation 1). Test model for the ANOVA including three factors

$$\boldsymbol{Y = B_0 + B_1 EAFS + B_2 VMR + B_3 EDAD + B_4 EAFS * VMR + B_5 EAFS * EDAD + B_6 VMR * AGE} \quad \textbf{(1)}$$

Where:
Y: compressive strength on cylinders (MPa)
B_i: coefficient of each of the effects, i=1,2,3,4,5,6
EAFS: percentage of slag in the cylinders, a number between 0 y 100
EDAD: cylinder age in days

The analysis of variance allowed building the model according to the effects that the experimental factors exert on the compressive strength. The results obtained from the ANOVA are presented in (Table 6).

Table 6. ANOVA three-factor model

Variable	Count	Suma of squares	Average of squares	F Value	Pr (>F)
EAFS	3	488.2	162.7	36.898	2.46e-06***
RGG	2	6.8	3.4	0.774	0.4828
AGE	2	2509.3	1254.6	284.479	7.77e-11***
EAFS:RGG	6	71	11.8	2.682	0.0688
EAFS:AGE	6	22.9	3.8	0.865	0.5471
RGG:AGE	4	3.3	0.8	0.186	0.9410
Residual		52.9	4.4		

Based on the results of (Table 6), it was observed that the EAFS and AGE factors are the most significant parameters on the compressive strength results, a situation that was visualized in the first approach by means of the boxplot plot (see (Figure 8)).

A new ANOVA was performed discarded the RGG factor since it neither significantly influence the behaviour on compressive strength or in the interaction between factors. The results are presented in (Table 7).

Table 7. ANOVA two-factor model

Variable	Count	Suma of squares	Average of squares	F Value	Pr (>F)
EAFS	3	488.2	162.7	31.11	2.43e-09***
AGE	2	2509.3	1254.6	239.89	<2e-16***
Residual	30	156.9	5.2		

The model obtained is presented in (Equation 2).

ANOVA Model for factors that influence the compressive strength.

$$\boldsymbol{Y = 14.2166 + 0.1198 * EAFS + 0.3935 * AGE} \quad \textbf{(2)}$$

Treatments with different effects were determined in the multiple comparisons test. (Figure 11) presents the main effects graph, which shows that the means of the compressive strength in the samples with replacements of 75 and 100% of coarse aggregate by EAFS are concentrated around 38 MPa, while the means in mixes with replacements of 25 and 50% of coarse aggregate by EAFS are around 30 MPa.

.

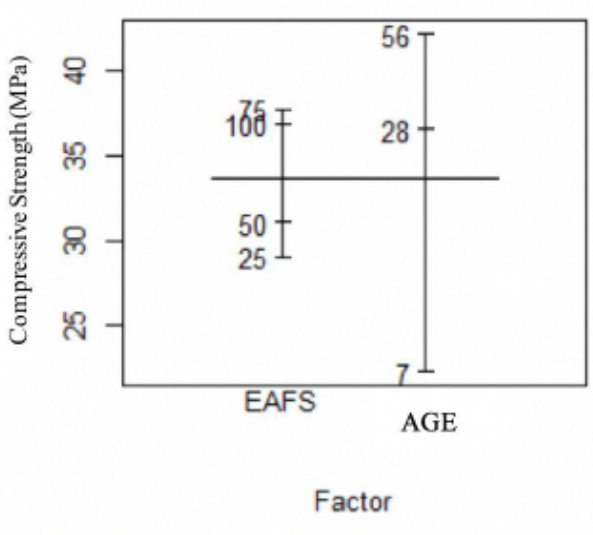

Figure 11. Main effects graph

(Figure 12) presents the EAFS-AGE interaction in which the development of compressive strength is observed in each EAFS substitution group over time, defining the mixture with 75% EAFS replacement as the one with the best performance (Pérez-Rojas et al., 2021b).

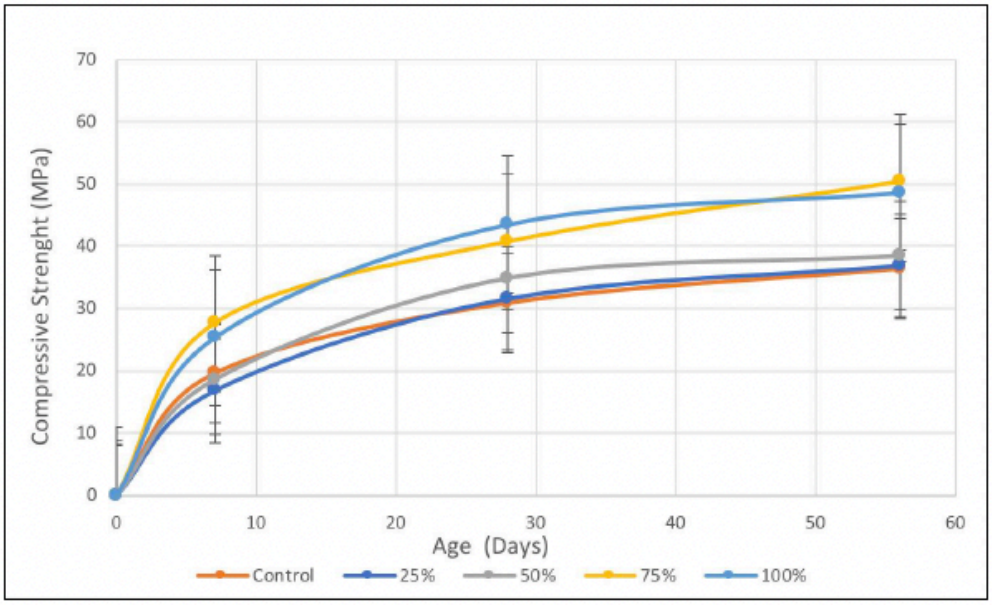

Figure 12. EAFS-AGE interaction

(Figure 13) presents the difference between means for the levels of EAFS and AGE, respectively.

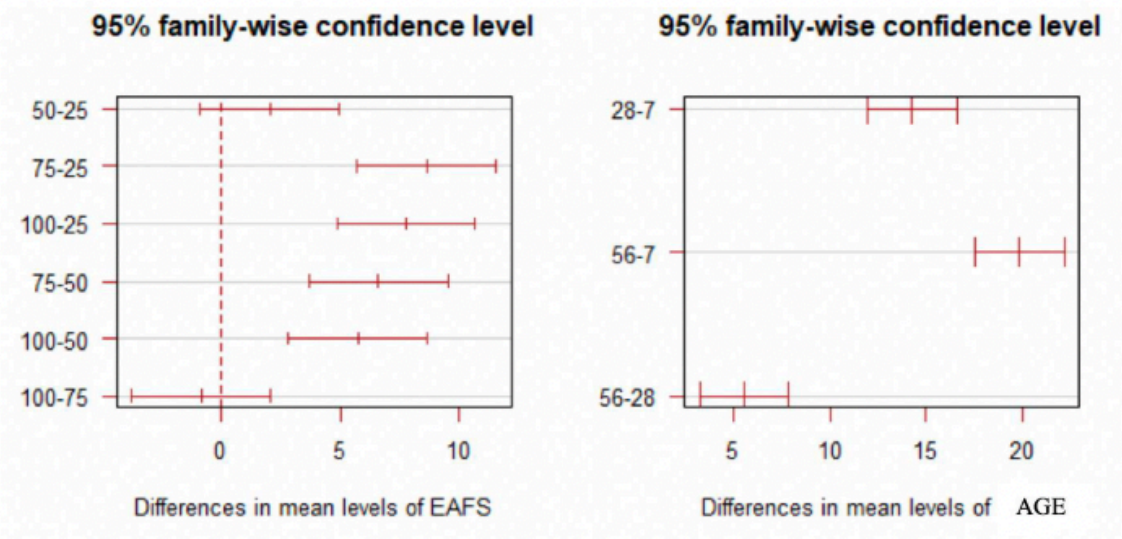

Figure 13. Difference between means for EAFS and AGE factors

In the difference of means for the levels of replacement of EAFS, it is observed that the value 0 belongs to two intervals, and it can be stablished that there are no significant differences between the compared means. In the difference of means for the AGE levels, it is observed that the value 0 does not belong to the intervals, therefore, it can be affirmed that there are significant differences between the compared means.

Since the sample with replacement of 75% EAFS presented a higher mean compression value at the three ages, it was chosen as the ideal replacement mixture. Hypothesis contrasts were performed between the mixtures with 75% EAFS replacement and the compressive strength of conventional concrete at each age. (Equation 3), (Equation 4), and (Equation 5) showed the hypothesis contrast of compressive strength at 7, 28, and 56 days respectively.

Hypothesis contrast of EAFS at 75% for age 7 days

$$\boldsymbol{H_0: \mu_{75\%} \geq 19,6}$$
$$\boldsymbol{H_a: \mu_{75\%} < 19,6} \quad \textbf{(3)}$$

Hypothesis contrast of EAFS at 75% for age 28 days

$$\boldsymbol{H_0: \mu_{75\%} \geq 30,9}$$
$$\boldsymbol{H_a: \mu_{75\%} < 30,9} \quad \textbf{(4)}$$

Hypothesis contrast of EAFS at 75% for age 56 days

$$\boldsymbol{H_0: \mu_{75\%} \geq 36,4}$$
$$\boldsymbol{H_a: \mu_{75\%} < 36,4} \quad \textbf{(5)}$$

Hypothesis testing was performed with the t-test, with a 95% confidence interval. The results obtained are presented in (Table 8).

Table 8. T-test to contrast the hypothesis of EAFS at 75% for ages 7, 28, and 56 days

Variable	df	Mean	T	p-value
7 days	2	25.7111	4.7946	0.9796
28 days	2	40.0666	8.9316	0.9938
56 days	2	47.2444	6.5235	0.9886

4.4 Corrosion Analysis by Electrochemical Impedance Spectroscopy

Once the significance of the EAFS variable in the compressive strength had been determined, neglecting the effects generated by RGG, the influence of these variables on corrosion resistance was studied.

For the study of corrosion in concrete mixtures, 25, 50, 75 and 100% of gravel was replaced by EAFS and simultaneously 40% of sand was replaced by RGG . Cylindrical concrete specimens of 10 cm diameter and 20 cm height were casted, with a smooth reinforcing rod of 1.27 cm diameter and 28 cm long embedded at the center of the specimen. (Figure 14) shows the test specimen.

Figure 14. Corrosion test specimens

The Gamry Instruments Framework 750 software was used to measure impedance. The software measures impedance between 10-3 mhz and 1 mhz and is capable of measuring impedance between 10-3 ω and1013ω. The potentiostat measures impedance by applying a sinusoidal voltage to the sample and measuring the current (Garmy Instruments, 2018). The presentation of the data and the analysis of these were done in Gamry Echem Analyst version 6.33.

The frequency range of the measurements ranged between 100 KHz and 10 MHz. Within a frequency decade 10 EIS measurements were taken, with an AC voltage signal of 10 mV.

The polarization resistance values for the reinforcing steel were estimated by adjusting the experimental impedance data taken with the Gamry Framework and the impedance results of the corresponding equivalent circuit (Saire, 2019).

The equivalent electronic circuit model is presented in (Figure 15).

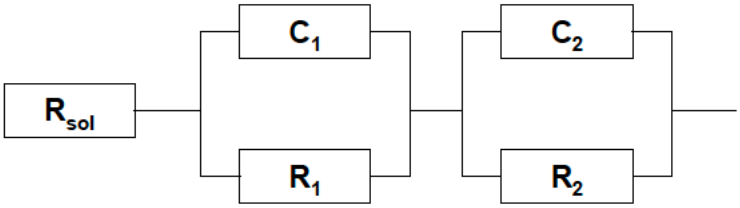

Figure 15. Electronic circuit model

According to (Ghanei et al., 2020), the impedance parameters of the model are:

Rsol: resistance due to solution of concrete pores (ohms) (Ω)
R1: concrete resistivity (ohms) (Ω)
C1: element phase constant (Farad) (F)
R2: load transfer resistance (ohms) (Ω)
C2: element capacitance phase constant (Farad) (F)

CPE is the constant of the phase angle of the element associated with the capacitance properties of the interface, or capacitance of the passive film formed (Saire, 2019).

The combination of the passive elements of the corrosion cell (resistances, capacitances, inductors), allowed to obtain the electrical parameters from which the speed and the corrosion mechanism were calculated (Flores et al., 2014).

The impedance parameters were measured in the set of mixtures and the results are presented in (Table 9).

Table 9. Electrical parameters of the equivalent circuit model

Mix	Rs (Ω)	CPEc (F)	Rc (Ω)	CPEdl (F)	Rct (Ω)
Control	744.3	1.79E-08	1314	8.12E-04	6579
M25	502.1	2.41E-08	1136	5.63E-04	5654
M50	434.6	4.63E-04	1979	3.60E-08	4876
M75	243.2	1.04E-08	1627	1.01E-03	3726
M100	280.3	1.36E-03	1876	4.12E-08	3546

According to (Sohail et al., 2020), concrete is a heterogeneous material and many intermingled interfacial regions contribute to the impedance spectra. These interfaces and the surface roughness of the electrode necessitate the constant phase element CPE to help match the circuit to the experimental spectra.
The total resistance of the circuit is made up of the resistance of the concrete, the resistance of the oxide product that has lime precipitation (Ca (OH) 2), and the resistance of the steel-concrete interface (Sohail et al., 2020). (Figure 16) presents the Nysquit plots for the samples tested at 150 days.

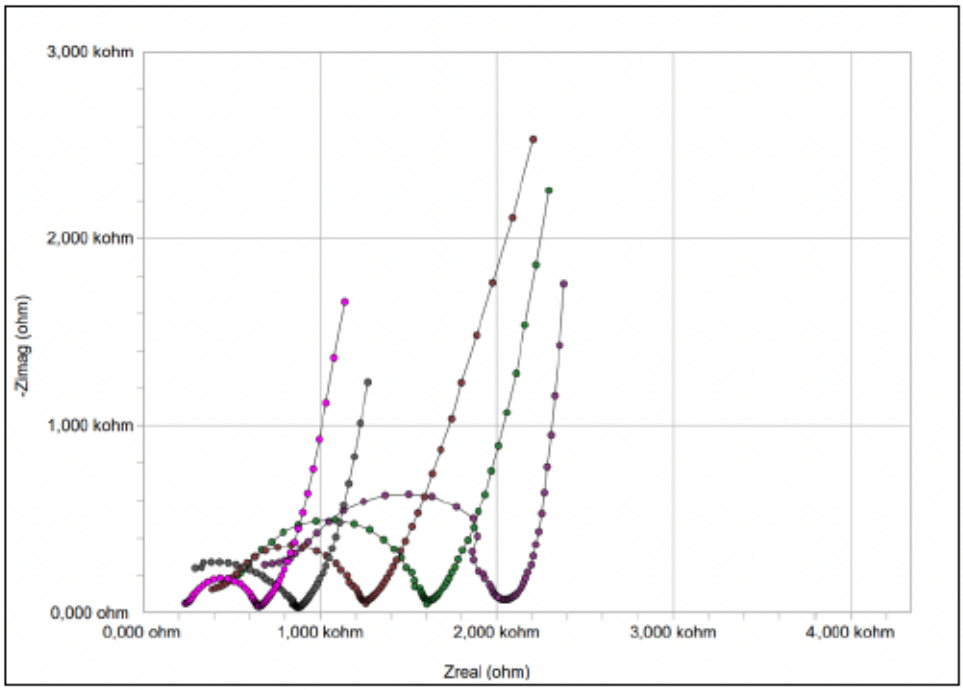

Figure 16. Nysquit plots for the samples tested at 150 days

The highest impedance according to (Figure 16) was presented by the standard sample, followed by the sample M25, M50, M75 and M100. The Nysquit impedance spectrum illustrates how increasing the percentage of EAFS reduces the impedance of the mixes.

Corrosion current density (icorr) measurements by EIS test are in the range of 0.6 and 0.13 μA/cm², the lowest of the measurements corresponding to the standard mixture sample.

The icorr measurements increased gradually with the increase in EAFS, compared to the standard mixture sample.Figure 17 shows the impedance spectrum obtained by the EIS technique for the set of samples. This behavior is due to the fact that the EIS test is influenced by the void content inside the specimen.

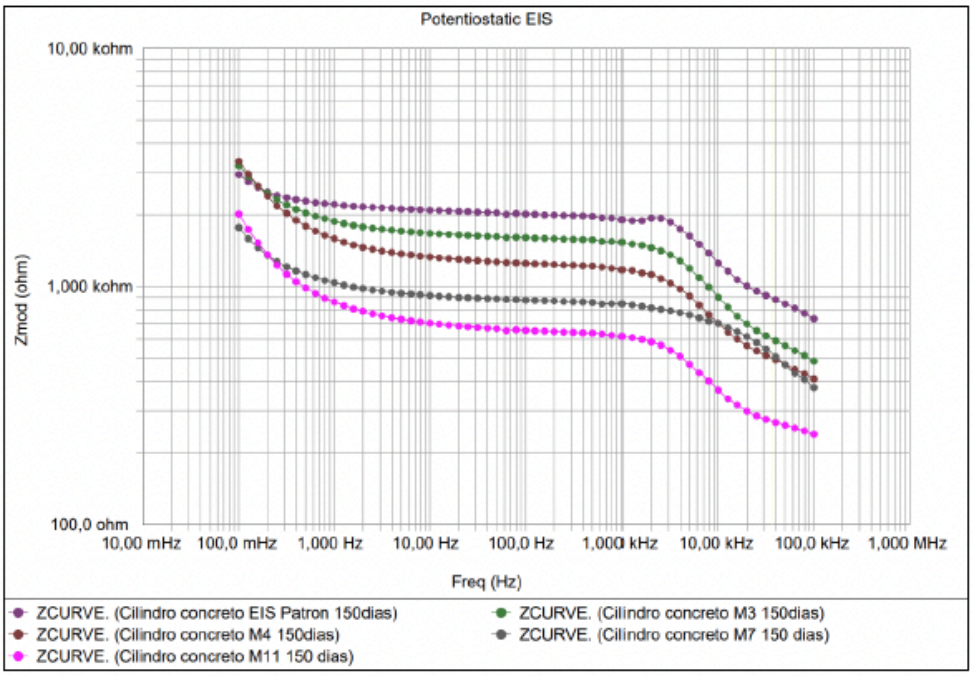

Figure 17. Bode impedance spectrum for the samples tested at 150 days

The CR (mm/y) increased as the content of EAFS increased in the concrete samples. However, the icorr values obtained indicate that the steels are in a passivation state.

Corrosion products in reinforcing steel are not expected to affect durability of EAFS replacement mixes.

5. Conclusions

The analysis of the physical and mechanical properties of natural aggregates (i.e., gravel and sand) and unconventional aggregates (i.e., EAFS and RGG), supports the simultaneous use of unconventional aggregates for the production of concrete mixtures, following the current INVIAS regulations.

The validity of the results obtained using the ACI 211.1 mixture design is confirmed. The strength adjustments suggested in step nine of the method are necessary.

The study proposed a w/c equal to 0.47 but in the verification by the expected design strength at 28 days, the w/c varied between 0.41 and 0.47.

According to multiple comparisons, it is found that mixtures with a replacement of 75% of gravel by EAFS present the highest value in the mean of compressive strength at different ages. Similarly, in the main effects graph, these mixtures present the highest average strength value.

The hypothesis test concludes that the average value of the compressive strength with a replacement of 75% of gravel by EAFS is higher than those specified for conventional concrete at each age and is chosen as the optimum replacement level.

The compressive strength results indicate that it is feasible to partially replace the natural gravel and sand by EAFS and RGG, respectively, reaching the specified strengths.

The mixes with replacements of EAFS and RGG will satisfactorily fulfill the life cycle of the project, without risk of failure due to corrosion of the reinforcing steel. Damage to concrete due to corrosion of reinforcing steel is not expected.

It is recommended to use the concrete mix with simultaneous replacements of gravel by EAFS in 75%, and sand by RGG in 40%, in the construction of rigid pavements in the department of Boyacá.

6. References

Adegoloye, G.; Beaucour, A.; Ortola, S.; Noumowe, A. (2016). Mineralogical composition of EAF slag and stabilised AOD slag aggregates and dimensional stability of slag aggregate concretes. Construction and Building Materials, 115, 171–178. https://doi.org/10.1016/j.conbuildmat.2016.04.036

Afshinnia, K.; Rangaraju, P. R. (2016). Impact of combined use of ground glass powder and crushed glass aggregate on selected properties of Portland cement concrete. Construction and Building Materials, 117, 263–272. https://doi.org/10.1016/j.conbuildmat.2016.04.072

Aprianti, E. (2016). A huge number of artificial waste material can be supplementary cementitious material (SCM) for concrete production. Review part II. Journal of Cleaner Production, 1–17.

Arribas, I.; Santamaría, A.; Ruiz, E.; Ortega-López, V.; Manso, J. M. (2015). Electric arc furnace slag and its use in hydraulic concrete. Construction and Building Materials, 90, 68–79. https://doi.org/10.1016/j.conbuildmat.2015.05.003

Ávila Díaz, M. Á.; Pinzón Galviss, S.; Serna Hernández, L. F. (2015). Análisis de curvas para el diseño de mezclas de concreto con material triturado del río Magdalena en el sector de Girardot, Cundinamarca. In Crescendo, 6(2), 136. https://doi.org/10.21895/incres.2015.v6n2.13

Flores, J.; Romero, R.; Genascá, J. (2014). Espectroscopía de Impedancia electroquímica en corrosión. In Journal of Chemical Information and Modeling. Retrieved from http://books.google.com/books?hl=en&lr=&id=cZDeh1W2nzEC&oi=fnd&pg=PA143&dq=Electrochemical+Impedance+Spectroscopy+and+its+Applications&ots=Ez6oI5xgmA&sig=HfXXx-xwhEq6nAf3jgnsclqaJpY%5Cnhttp://link.springer.com/10.1007/0-306-46916-2_2%5Cnhttp://depa.fquim.

Garmy Instruments. (2018). Electrochemical Impedance Spectroscopy Software. https://doi.org/10.1002/9781118684030.ch14

Ghanei, A.; Eskandari-Naddaf, H.; Ozbakkaloglu, T.; Davoodi, A. (2020). Electrochemical and statistical analyses of the combined effect of air-entraining admixture and micro-silica on corrosion of reinforced concrete. Construction and Building Materials, 262. https://doi.org/10.1016/j.conbuildmat.2020.120768

Giraldo Bolivar, O. (2006). Dosificación de mezclas de hormigón. Medellín, CO.

Girardo Bolívar, O. (1987). Guía práctica para el diseño de mezclas de hormigón. Medellín, CO.

Gong, C.; Zhang, J.; Wang, S.; Lu, L. (2015). Effect of aggregate gradation with fuller distribution on properties of sulphoaluminate cement concrete. Journal Wuhan University of Technology, Materials Science Edition, 30(5), 1029–1035. https://doi.org/10.1007/s11595-015-1268-5

INVIAS. Instituto Nacional de Vías. (2012) Normas y Especificaciones. Capítulo 5 Pavimentos de concreto.

INVIAS. Instituto Nacional de Vías. (2012). Resistencia a la compresión de cilindros de concretos.

Ling, T. C.; Poon, C. S.; Wong, H. W. (2013). Management and recycling of waste glass in concrete products: Current situations in Hong Kong. Resources, Conservation and Recycling, 70, 25–31. https://doi.org/10.1016/j.resconrec.2012.10.006

Muhmood, L.; Vitta, S.; Venkateswaran, D. (2009). Cementitious and pozzolanic behavior of electric arc furnace steel slags. Cement and Concrete Research, 39(2), 102–109. https://doi.org/10.1016/j.cemconres.2008.11.002

Nassar, R. U. D.; Soroushian, P. (2012). Strength and durability of recycled aggregate concrete containing milled glass as partial replacement for cement. Construction and Building Materials, 29, 368–377. https://doi.org/10.1016/j.conbuildmat.2011.10.061

Omran, A.; Tagnit-Hamou, A. (2016). Performance of glass-powder concrete in field applications. Construction and Building Materials, 109, 84–95.

Pérez-Rojas, Y. A.; Vera-López, E.; Ochoa-Díaz, R. (2021a). Morphological , chemical , and mineralogical characterization of concrete mixtures produced by electric arc furnace slag Morphological , chemical , and mineralogical characterization of concrete mixtures produced by electric arc furnace slag. Journal of Physics: Conference Series, 2046(1), 012035. https://doi.org/10.1088/1742-6596/2046/1/012035

Pérez-Rojas, Y. A.; Vera-López, E.; Ochoa-Díaz, R. (2021b). Optimal performance of concrete produced by electric arc furnace slag and recycled ground glass in pavement construction. Journal of Physics: Conference Series, 2046(1), 012034. https://doi.org/10.1088/1742-6596/2046/1/012034

Pérez, Y.; Vera, E.; Diaz, J.; López, M. (2017). Preparation of concrete mixtures with electric arc furnace slag and recycled ground glass. Journal of Physics: Conference Series, 935(1). https://doi.org/10.1088/1742-6596/935/1/012010

Rajagopal, A. S.; Veeraragavan, A.; Justo, C. E. G. (1984). A simplified approach for mix design based on shape factors of coarse aggregates. Bulletin of the International Association of Engineering Geology, 30(1), 123–126. https://doi.org/10.1007/bf02594292

Reddy, M. S.; Dinakar, P.; Rao, B. H. (2018). Mix design development of fly ash and ground granulated blast furnace slag based geopolymer concrete. Journal of Building Engineering, 20, 712–722. https://doi.org/10.1016/j.jobe.2018.09.010

Rivera, G. (2013). Concreto simple. Cali, CO.

Romero, A. F.; Hernández, J. C. (2014). Diseño de mezclas de hormigón por el método A.C.I. y efectos de la adición de cenizas volantes de Termotasajero en la resistencia a la compresión (Universidad Santo Tomás). https://doi.org/10.1117/12.742328

Rondi, L.; Bregoli, G.; Sorlini, S.; Cominoli, L. (2016). Concrete with EAF steel slag as aggregate: A comprehensive technical and environmental characterisation. Composites Part B: Engineering, 90, 195–202. https://doi.org/10.1016/j.compositesb.2015.12.022

Saire, J. (2019). Morphology and Detection of Corrosion on Stainless Steel Reinforcement in Concrete (University of South Florida). Retrieved from https://scholarcommons.usf.edu/etd/7922

Sohail, M. G.; Kahraman, R.; Alnuaimi, N. A.; Gencturk, B.; Alnahhal, W.; Dawood, M.;Belarbi, A. (2020). Electrochemical behavior of mild and corrosion resistant concrete reinforcing steels. Construction and Building Materials, 232(117205). https://doi.org/10.1016/j.conbuildmat.2019.117205

Sumayya, M.; Romeela, M.; Prakash, K. (2016). Characterisation of electric arc furnace slags as concrete aggregate.pdf. Construction and Building Materials, 105, 459–464.

Yanez, J. (2019). Morphology and Detection of Corrosion on Stainless Steel Reinforcement in Concrete (University of South Florida). Retrieved from https://scholarcommons.usf.edu/etd/7922.